Sensors and Actuators B 197 (2014) 172–176

Contents lists available at ScienceDirect

Sensors and Actuators B: Chemical

journal homepage: www.elsevier.com/locate/snb

Highly selective and sensitive colorimetric detection of Ag(I) using *N*-1-(2-mercaptoethyl)adenine functionalized gold nanoparticles

Yi-Ming Sung, Shu-Pao Wu *

Department of Applied Chemistry, National Chiao Tung University, Hsinchu, Taiwan

ARTICLE INFO

Article history:
Received 26 December 2013
Received in revised form 11 February 2014
Accepted 11 February 2014
Available online 5 March 2014

Keywords:
Colorimetric sensor
Ag^+
Gold nanoparticles
Adenine

ABSTRACT

A sensitive and selective colorimetric Ag^+ detection method was developed by using *N*-1-(2-mercaptoethyl)adenine functionalized gold nanoparticles (MEA-AuNPs). The presence of Ag^+ immediately induced aggregation of MEA-AuNPs, yielding a color change from red to blue. This Ag^+-induced aggregation of MEA-AuNPs was monitored by bare eye and UV–vis spectroscopy with a detection limit of 3.3 nM. MEA-AuNPs showed excellent selectivity toward Ag^+ compared with other metal ions through interaction between adenine and Ag^+. The best detection of Ag^+ was achieved at pH 6–9. Furthermore, MEA-AuNPs were applied to detect Ag^+ in lake water with low interference.

1. Introduction

The development of rapid and efficient detection of metal ions in environmental and biological systems has been an important research issue. Silver compounds are widely used in the electrical, photographic, and imaging industry [1,2]. Because of heavy use in industry, a massive quantity of Ag is released to the environment annually. Silver ions bind with amine, imidazole, carboxylate, and thiol groups in proteins, resulting in loss of protein functions [3,4]. Additionally, silver nanoparticles can generate reactive oxygen species and destroy aqueous organisms by inhibiting their growth and interrupting their reproductive ability [5,6].

Traditional methods such as atomic absorption spectrometry [7], inductively coupled plasma-atomic emission spectrometry [8,9], and voltammetry [10,11] have been developed for measuring silver ions in biological and environmental samples. Although these methods are quantitative, they require sophisticated apparatus and tedious sample pretreatment prior to metal species analysis. Recently, researchers have focused on the development of sensitive and selective sensors for silver ion determination.

Gold nanoparticles (AuNPs) have been widely used in the development of colorimetric probes for detecting metal ions [12–20], anions [21,22], and biomolecules [23,24] because of their unique optical properties. AuNPs display strong surface plasmon resonance (SPR) absorption properties, which are extremely sensitive to size, shape, and interparticle distance [25,26]. AuNP-based colorimetric sensors utilize interparticle plasmon coupling on analyte-induced aggregation of AuNPs, which results in a color change from red to blue. In these assays, analyte-triggered aggregation of AuNPs leads to a wine-red shift in the SPR absorption band, resulting in a red-to-blue color change. The analyte-triggered aggregation of AuNPs relies on modification of the surface of the AuNPs that can specifically recognize target species. Appropriate surface functionalization of AuNPs will determine the analytical applicability and selectivity of AuNPs.

In this report, adenine-functionalized AuNPs (MEA-AuNPs) were synthesized to detect Ag^+. Adenine showed excellent coordination with Ag^+ to form Adenine–Ag^+–Adenine complexes through a bond between the nitrogen atoms on adenine with Ag^+ [27–31]. AuNPs were prepared through citrate-mediated reduction of $HAuCl_4$. *N*-1-(2-mercaptoethyl)adenine (MEA) was attached to the surface of AuNPs through the thiol group, and MEA-AuNPs were used for metal ion detection. Metal ions such as Ag^+, Al^{3+}, Ca^{2+}, Cd^{2+}, Co^{2+}, Cu^{2+}, Cr^{3+}, Fe^{2+}, Fe^{3+}, Hg^{2+}, K^+, Mg^{2+}, Mn^{2+}, Na^+, Ni^{2+}, Pb^{2+}, and Zn^{2+} were tested for metal ion selectivity. However, Ag^+ was the only metal ion that caused the aggregation of MEA-AuNPs. This caused the SPR absorption band of the MEA-AuNPs to shift to a longer wavelength, and consequently led to a color change from red to blue. This color change can be used to detect the presence of Ag^+ ions. SPR absorption at 650 nm directly indicates the degree of MEA-AuNP aggregation caused by the addition of Ag^+ ions.

* Corresponding author. Tel.: +886 3 5712121x56506; fax: +886 3 5723764.
E-mail addresses: spwu@mail.nctu.edu.tw, spwu@faculty.nctu.edu.tw (S.-P. Wu).

http://dx.doi.org/10.1016/j.snb.2014.02.044
0925-4005/

2. Experimental

2.1. Chemicals

Hydrogen tetrachloroaurate(III) tetrahydrate, citric acid, KCl and NaCl were purchased from Showa. Adenine, ethylene carbonate, solid potassium thioacetate, $Al(ClO_4)_3{\cdot}9H_2O$, $Cr(ClO_4)_3{\cdot}6H_2O$ and trisodium citrate were purchased from Alfa Aesar. $AgClO_4{\cdot}xH_2O$, $Ca(ClO_4)_2{\cdot}4H_2O$, $Cd(ClO_4)_2{\cdot}xH_2O$, $CoCl_2{\cdot}6H_2O$, $Cu(BF_4)_2{\cdot}xH_2O$, $Fe(BF_4)_2$, $FeCl_3{\cdot}6H_2O$, $Hg(ClO_4)_2{\cdot}xH_2O$, $Mg(ClO_4)_2{\cdot}6H_2O$, $Ni(O_2CCH_3){\cdot}4H_2O$, $Pb(ClO_4)_2{\cdot}3H_2O$ and $Zn(BF_4)_2{\cdot}xH_2O$ were purchased from Sigma–Aldrich. $MnSO_4{\cdot}H_2O$ were purchased from Riedel-de Haen. 4-(2-Hydroxyethyl)-1-piperazine-ethane-sulfonic acid (Hepes) and tris(hydroxymethyl) aminomethane (Tris) were purchased from Biobasic. 2-(N-morpholino)ethanesulfonic acid (Mes) was purchased from J.T. Baker. For all aqueous solutions, deionized water (resistivity, 18.0 MΩ cm at 25 °C) purified by Millipore Direct-Q water purification unit was used. The synthesis and characterization of *N*-1-(2-mercaptoethyl)adenine (MEA) are described in the supporting information [32].

2.2. Instruments

UV-vis spectras were recorded on an Agilent 8453 UV-vis spectrometer (Santa Clara, CA, USA). TEM images were recorded from JEOL JEM-2010 Transmission Electro Microscope (Tokyo, Japan). IR data were obtained on BomemDA8.3 Fourier-Transform Infrared Spectrometer (Quebec, Canada). ICP-MS data were recorded on an ICP-MS Perkin Elmer SCIEX ELAN 5000 (Waltham, MA, USA).

2.3. Preparation of MEA-AuNPs

Gold nanoparticles were prepared by reducing $HAuCl_4$ with trisodium citrate. All glassware was thoroughly cleaned with aqua regia (3:1, HCl/HNO_3) and rinsed with Millipore-Q water prior to use. Briefly, $HAuCl_4$ (40 mL, 195 μM) was heated to 80 °C. Trisodium citrate solution (540 μL, 0.1 M) was added rapidly to the solution and the mixture solution was heated for 2 h at the same temperature. In order to remove excess sodium citrate, the citrate-reduced Au nanoparticles were centrifuged for 15 min (12000 rpm) and then dissolved with Millipore-Q water. *N*-1-(2-mercaptoethyl)adenine (MEA) solution (1.2 mL, 0.05 mM, in H_2O-DMSO (v/v = 200:1) was incubated with AuNPs solution for 3 h. Excess MEA was removed by dialysis 3.5 K MWCO Spectra/Por 7 membranes. The finally dispersed MEA-AuNPs can be used for metal ions detection. The sizes of the MEA-AuNPs were verified by transmission electron microscope (TEM) analysis.

2.4. Colorimetric detection of Ag^+

To a 1.0 mL of solution containing MEA-AuNPs, different metal ions (4 μM): Ag^+, Al^{3+}, Ca^{2+}, Cd^{2+}, Co^{2+}, Cr^{3+}, Cu^{2+}, Fe^{2+}, Fe^{3+}, Hg^{2+}, K^+, Mg^{2+}, Mn^{2+}, Na^+, Ni^{2+}, Pb^{2+}, and Zn^{2+} were added separately. The mixtures were maintained at room temperature for 20 min and then transferred separately into 1.5-mL quartz cuvette. Their SPR absorption bands were recorded by UV–vis spectrophotometer.

2.5. The influence of pH on Ag^+ induced aggregation of MEA-AuNPs

MEA-AuNPs were added with Ag^+ (30 μM) in 1.0 mL water solution (10 mM buffer). The buffers were: pH 3–4, $CH_3COOH/NaOH$; pH 4.5–7.0, MES; pH 7.0–10, Hepes.

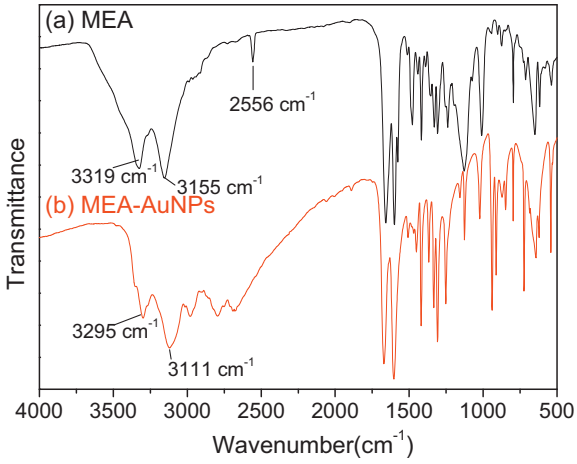

Fig. 1. FT-IR spectra of MEA and MEA-AuNPs.

3. Results and discussion

3.1. Characterization of MEA-AuNPs

AuNPs were prepared through citrate-mediated reduction of $HAuCl_4$. MEA, the capping agent, was added to the AuNP solution. The transmission electron microscopy (TEM) image reveal that the particle size of MEA-AuNPs ranged from 15 nm to 23 nm, with most particle sizes falling in the range of 19–21 nm. MEA-AuNPs were also characterized by using infrared spectroscopy. As shown in Fig. 1a, the characteristic skeleton peaks of MEA were 3319 cm^{-1} (N—H), 3155 cm^{-1} (N—H), and 2556 cm^{-1} (S—H). In Fig. 1b, the peak that was originally at 2556 cm^{-1} (S—H) disappeared, indicating that MEA binds to AuNPs via the Au–S bond [33]. SPR absorption of AuNPs was measured by using a UV–vis spectrophotometer, and its maximum absorption was located at 530 nm.

3.2. Interaction of MEA-AuNPs with various metal ions

The bonding performance of MEA-AuNPs with metal ions in aqueous solutions was tested. To evaluate the selectivity of MEA-AuNPs toward various metal ions, the absorption spectra of MEA-AuNPs were obtained in the presence of several metal ions: Ag^+, Al^{3+}, Ca^{2+}, Cd^{2+}, Co^{2+}, Cr^{3+}, Cu^{2+}, Fe^{2+}, Fe^{3+}, Hg^{2+}, K^+, Mg^{2+}, Mn^{2+}, Na^+, Ni^{2+}, Pb^{2+}, and Zn^{2+}. Fig. 2 shows the effect of metal ions on the appearance of MEA-AuNPs in solution. Ag^+ was the only ion that resulted in an absorption peak shift from 530 nm to 650 nm. This red shift could also be observed by bare eye as a color change from red to blue. Other metal ions did not influence the absorption spectra, indicating that no aggregation occurred. The adenine groups on MEA-AuNPs function as ligands binding metal ions. Since Ag^+ was bound between the adenines, the MEA-AuNPs aggregated (Fig. 3).

The reaction of MEA-AuNPs with Ag^+ was fast; addition of Ag^+ (aq) to the solution of MEA-AuNPs caused an immediate change in absorbance (see Fig. S5 in the supporting information). To gain a clearer understanding of the interaction between Ag^+ and MEA-AuNPs, ^1H NMR spectroscopy was employed (see Fig. S6 in the supporting information). The ^1H NMR spectra of 9-(2-hydroxyethyl)-6-amino-9H-purine recorded with increasing amounts of Ag^+ show that the amine proton signal (H_c) at $\delta = 7.20$ ppm was shifted downfield as Ag^+ was added. The proton signals (H_a, H_b) at $\delta = 8.15$, 8.05 ppm were also shifted downfield. These observations indicate that Ag^+ interacts with adenine mainly through one amine and one nitrogen atom in adenine. Ag^+-triggered aggregation of MEA-AuNPs occurred mainly through

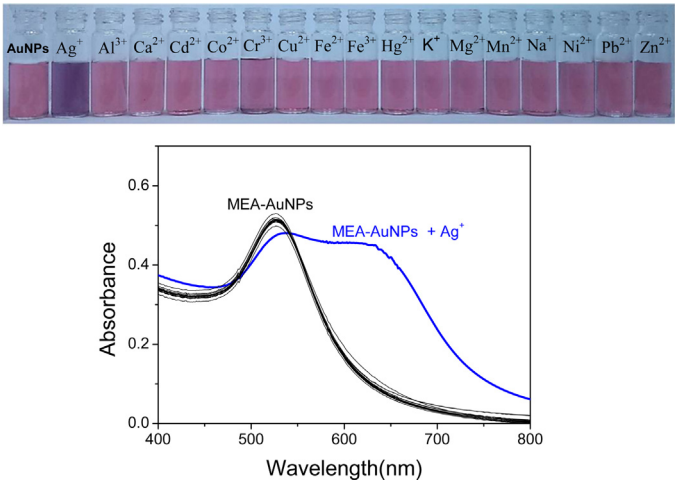

Fig. 2. (Top) Photographics of MEA-AuNPs in the presence of various metal ions (4 μM). (Bottom) UV–vis spectra of MEA-AuNPs in the presence of different metal ions (4 μM). Buffer: 5 mM Hepes, pH 7.5.

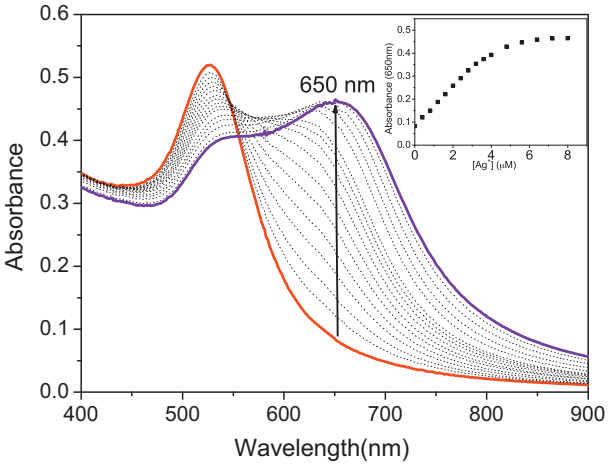

Fig. 4. Change in surface plasmon resonance absorption of MEA-AuNPs in the presence of different concentrations of Ag^+.

two-step binding. The first step involves MEA binding to a Ag^+ ion through nitrogen atoms in adenine. Second, bonds formed between Ag^+ and nitrogen atoms in another MEA molecule capping adjacent AuNPs, resulting in aggregation. Fig. 3c shows the TEM image of Ag^+-induced aggregation of MEA-AuNPs. Effectively, Ag^+ functioned as a bridge between particles and triggered the aggregation of MEA-AuNPs.

The degree of aggregation of MEA-AuNPs depended on the concentration of Ag^+ ions; Fig. 4 shows the change in SPR absorption with the addition of different concentrations of Ag^+. The absorbance at 530 nm decreased with increasing Ag^+ concentration. A new band at 650 nm formed during Ag^+ titration as a result of the induced aggregation of AuNPs. A linear relationship was found when the concentration of Ag^+ ions was between 0 and 4 μM. The limit of detection for Ag^+ was found to be 3.3 nM (see Fig. S7 in the

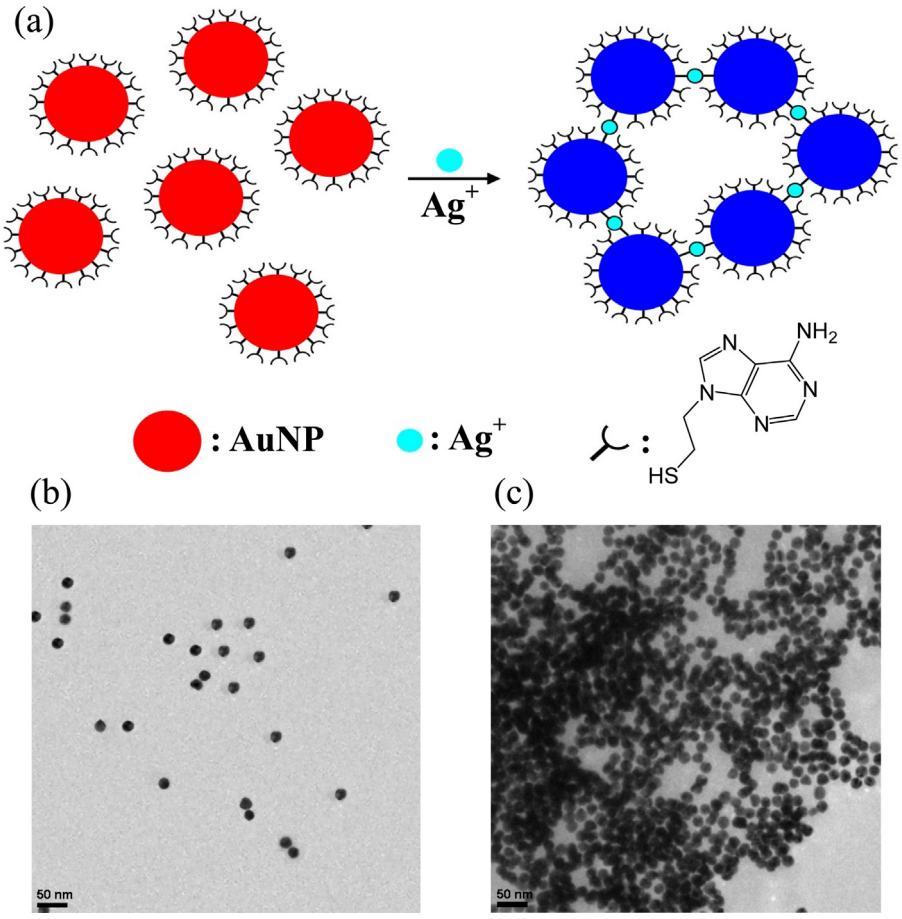

Fig. 3. (a) Depiction of the Ag^+-triggered aggregation of MEA-AuNPs for Ag^+ detection. (b) TEM image of MEA-AuNPs. (c) TEM image of MEA-AuNPs in the presence of Ag^+. Scale bar is 50 nm.

Table 1
Comparison of this work with some methods for Ag^+ detection.

Detection method	Linear range (*M*)	Limit of detection (*M*)	Reference
AA	9.3×10^{-7}–7.5×10^{-6}	5.6×10^{-9}	[7]
ICP-AES	9.3×10^{-7}–8.4×10^{-6}	1.9×10^{-7}	[8]
Voltammetry	1.0×10^{-9}–1.0×10^{-4}	1.0×10^{-9}	[10]
Colorimetric probe	6.4×10^{-8}–2.4×10^{-7}	3.2×10^{-8}	[34]
Ratiometricfluorescent probe	0–7.5×10^{-5}	3.4×10^{-7}	[35]
This method	0–4.0×10^{-6}	3.3×10^{-9}	

supporting information), which is lower than those of previously reported optical assays as shown in Table 1.

Aggregated MEA-AuNPs can be redispersed by removing Ag^+ ions with EDTA; this was confirmed by the consequent SPR absorption shift from 650 nm to 530 nm (Fig. 5). After the solution was removed by using a centrifuge and after it was suspended with aqueous media, the dispersed MEA-AuNPs could be reused to detect Ag^+ (see Fig. S8 in the supporting information). Through this technique, the MEA-AuNP system can be used repeatedly for the detection of Ag^+.

3.3. Interference studies

In order to study the influence of other metal ions on Ag^+ binding to MEA-AuNPs, competitive experiments were carried out in the presence of Ag^+ (4 μM) and other metal ions Al^{3+}, Ca^{2+}, Cd^{2+}, Co^{2+}, Cr^{3+}, Cu^{2+}, Fe^{2+}, Fe^{3+}, Hg^{2+}, K^+, Mg^{2+}, Mn^{2+}, Na^+, Ni^{2+}, Pb^{2+}, and Zn^{2+} (Fig. 6). The SPR absorption shift caused by the mixture of Ag^+ with another metal ion was similar to that caused solely by Ag^+. This indicates that other metal ions did not interfere in the binding of MEA-AuNPs with Ag^+. This finding is consistent with previous studies, suggesting that Ag^+ is the only metal ion that can induce the aggregation of MEA-AuNPs.

3.4. The influence of pH on Ag^+-induced aggregation of MEA-AuNPs

To investigate the pH range in which MEA-AuNPs can effectively detect Ag^+, pH titration of MEA-AuNPs was carried out. In Fig. 7, the absorbance ratio (A_{650}/A_{530}) of MEA-AuNPs was low and constant in the pH range 6–12. This indicates that MEA-AuNPs were stable in the pH range 6–12. When the pH was lower than 6, the absorbance ratio (A_{650}/A_{530}) of MEA-AuNPs significantly increased. Under acidic conditions (pH < 6), protonation of adenine resulted in the aggregation of AuNPs. The influence of pH on Ag^+-induced aggregation of MEA-AuNPs is shown in Fig. 7; addition of Ag^+ resulted in a high absorbance ratio (A_{650}/A_{530}) at pH 4–9. At pH > 9,

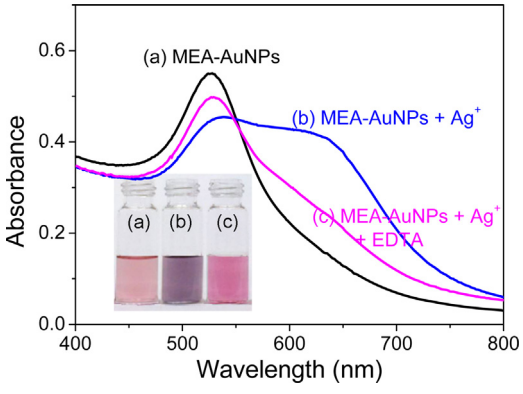

Fig. 5. Reversible binding of Ag^+ to MEA-AuNPs. UV–vis spectra of (a) MEA-AuNPs, (b) MEA-AuNPs in the presence of Ag^+ (4 μM), and (c) MEA-capped AuNPs in the presence of Ag^+ (4 μM) upon addition of EDTA (1 mM).

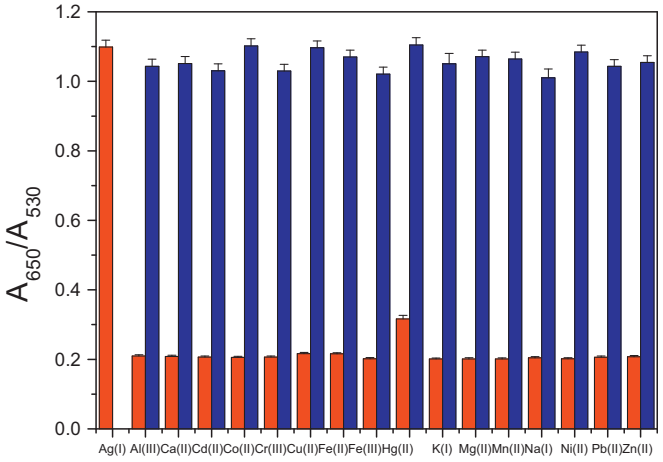

Fig. 6. Absorbance ratio (A_{650}/A_{530}) of MEA AuNPs in the presence of metal ions. Red bars represent the addition of single metal ion (200 μM); blue bars represent the mixture of Ag^+ (4 μM) with another metal ion (200 μM).

the absorbance ratio (A_{650}/A_{530}) decreased because of formation of colloidal Ag_2O [36]. Therefore, the optimal pH range for detecting Ag^+ by MEA-AuNPs is in the pH range of 6–9.

3.5. Application of MEA-AuNPs for the analysis of lake water samples

To confirm the practical application of MEA-AuNPs, water sample from the lake located in NCTU, Hsinchu, Taiwan, was collected and spiked with different amounts of Ag^+ standard solution. A calibration curve of MEA-AuNP absorbance ratio (A_{650}/A_{530}) in the presence of different concentrations of Ag^+ was prepared (Fig. S6 in the supporting information). Analytical results are shown in Table 2. The recovery values ranged from 95.5% to 103.5% with the relative standard deviation (RSD) lower than 3.2%. The results

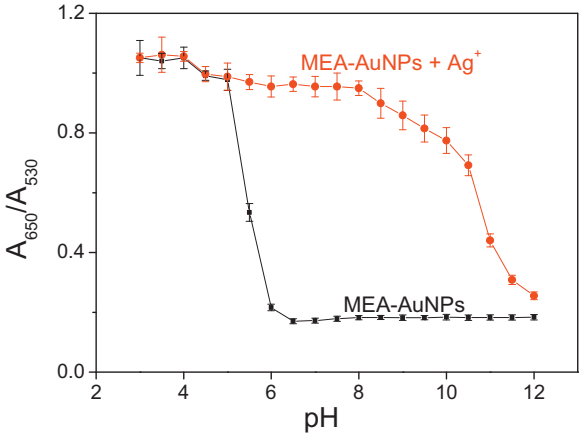

Fig. 7. Influence of pH on the UV–vis spectra of MEA-AuNPs in the absence and presence of Ag^+ (4 μM).

Table 2
Determination of Ag^+ in lake water.

Sample	Added Ag^+ (μM)	Proposed method (μM)	Recovery (%)	RSD (n = 3, %)	ICP-MS method (μM)
1	1.0	1.0	96.6	3.2	1.0
2	2.0	2.0	103.5	1.8	2.1
3	3.0	2.9	95.5	1.7	3.2

obtained with MEA-AuNPs are in good agreement with those obtained by ICP-MS. These results demonstrate that the designed probe is applicable to detection of Ag^+ in lake water samples.

4. Conclusion

In summary, new MEA-AuNPs have been developed for colorimetric sensing of Ag^+ ions. The functionalized AuNPs for colorimetric sensing of Ag^+ exhibited high selectivity in the presence of other interfering metal ions. This color assay offers a fast method for monitoring Ag^+ at a low cost and allows detection of concentrations as low as 3.3 nM. The optimal pH range for Ag^+ detection using MEA-AuNPs was determined to be 6–9. The color assay was also applied in the analysis of Ag^+ in lake water, with recovery ranging from 95.5% to 103.5%.

Acknowledgements

We gratefully acknowledge the financial support of the National Science Council Taiwan and National Chiao Tung University.

Appendix A. Supplementary data

Supplementary data associated with this article can be found, in the online version, at http://dx.doi.org/10.1016/j.snb.2014.02.044.

References

[1] H.T. Ratte, Bioaccumulation and toxicity of silver compounds: a review, Environ. Toxicol. Chem. 18 (1999) 89–108.
[2] J.L. Barriada, A.D. Tappin, E.H. Evans, E.P. Achterberg, Dissolved silver measurements in seawater, Trends Anal. Chem. 26 (2007) 809–817.
[3] S. Liau, D. Read, W. Pugh, J. Furr, A. Russell, Interaction of silver nitrate with readily identifiable groups: relationship to the antibacterialaction of silver ions, Lett. Appl. Microbiol. 25 (1997) 279–283.
[4] T.N. Wells, P. Scully, G. Paravicini, A.E. Proudfoot, M.A. Payton, Mechanism of irreversible inactivation of phosphomannose isomerases by silver ions and flamazine, Biochemistry 34 (1995) 7896–7903.
[5] C. Carlson, S. Hussain, A. Schrand, L.K. Braydich-Stolle, K. Hess, R. Jones, J. Schlager, Unique cellular interaction of silver nanoparticles: size-dependent generation of reactive oxygen species, J. Phys. Chem. B 112 (2008) 13608–13619.
[6] P. AshaRani, G. Low Kah Mun, M.P. Hande, S. Valiyaveettil, Cytotoxicity and genotoxicity of silver nanoparticles in human cells, ACS Nano 3 (2008) 279–290.
[7] Q. Pu, Q. Sun, Application of 2-mercaptobenzothiazole-modified silica gel to on-line preconcentration and separation of silver for its atomic absorption spectrometric determination, Analyst 123 (1998) 239–243.
[8] A. Väisänen, R. Suontamo, J. Silvonen, J. Rintala, Ultrasound-assisted extraction in the determination of arsenic, cadmium, copper, lead, and silver in contaminated soil samples by inductively coupled plasma atomic emission spectrometry, Anal. Bioanal. Chem. 373 (2002) 93–97.
[9] M. Hosoba, K. Oshita, R.K. Katarina, T. Takayanagi, M. Oshima, S. Motomizu, Synthesis of novel chitosan resin possessing histidine moiety and its application to the determination of trace silver by ICP-AES coupled with triplet automated-pretreatment system, Anal. Chim. Acta 639 (2009) 51–56.
[10] A. Ceresa, A. Radu, S. Peper, E. Bakker, E. Pretsch, Rational design of potentiometric trace level ion sensors. A Ag^+-selective electrode with a 100 ppt detection limit, Anal. Chem. 74 (2002) 4027–4036.
[11] X.-B. Zhang, Z.-X. Han, Z.-H. Fang, G.-L. Shen, R.-Q. Yu, 5,10, 15-Tris (pentafluorophenyl) corrole as highly selective neutral carrier for a silver ion-sensitive electrode, Anal. Chim. Acta 562 (2006) 210–215.
[12] Y. Chen, I. Lee, Y. Sung, S. Wu, Triazole functionalized gold nanoparticles for colorimetric Cr^{3+} sensing, Sens. Actuators B 188 (2013) 354–359.
[13] E. Tan, P. Yin, X. Lang, X. Wang, T. You, L. Guo, Functionalized gold nanoparticles as nanosensor for sensitive and selective detection of silver ions and silver nanoparticles by surface-enhanced Raman scattering, Analyst 137 (2012) 3925–3928.
[14] P. Miao, L. Ning, X. Li, Gold nanoparticles and cleavage-based dual signal amplification for ultrasensitive detection of silver ions, Anal. Chem. 85 (2013) 7966–7970.
[15] B. Liu, H. Tan, Y. Chen, Visual detection of silver (I) ions by a chromogenic reaction catalyzed by gold nanoparticles, Microchimica Acta 180 (2013) 331–339.
[16] L. Chen, T. Lou, C. Yu, Q. Kang, L. Chen, N-1-(2-Mercaptoethyl)thymine modification of gold nanoparticles: a highly selective and sensitive colorimetric chemosensor for Hg2+, Analyst 136 (2011) 4770–4773.
[17] T. Lou, Z. Chen, Y. Wang, L. Chen, Blue-to-red colorimetric sensing strategy for Hg^{2+} and Ag via redox-regulated surface chemistry of gold nanoparticles, ACS Applied Materials & Interfaces 3 (2011) 1568–1573.
[18] T. Lou, L. Chen, C. Zhang, Q. Kang, H. You, D. Shen, L. Chen, A simple and sensitive colorimetric method for detection of mercury ions based on anti-aggregation of gold nanoparticles, Anal. Methods 4 (2012) 488–491.
[19] H. Tan, B. Liu, Y. Chen, Effects of the electrostatic repulsion between nanoparticles on colorimetric sensing: an investigation of determination of Hg^{2+} with silver nanoparticles, Plasmonics 8 (2013) 705–713.
[20] S. Bothra, J.N. Solanki, S.K. Sahoo, Functionalized silver nanoparticles as chemosensor for pH, He^{2+} and Fe^{3+} in aqueous medium, Sens. Actuators B 188 (2013) 937–943.
[21] W.L. Daniel, M.S. Han, J.S. Lee, C.A. Mirkin, Colorimetric nitrite and nitrate detection with gold nanoparticle probes and kinetic end points, J. Am. Chem. Soc. 131 (2009) 6362–6363.
[22] Z. Zhang, J. Zhang, C. Qu, D. Pan, Z. Chen, L. Chen, Label free colorimetric sensing of thiocyanate based on inducing aggregation of Tween 20-stabilized gold nanoparticles, Analyst 137 (2012) 2682–2686.
[23] C.A. Mirkin, R.L. Letsinger, R.C. Mucic, J.J. Storhoff, A DNA-based method for rationally assembling nanoparticles into macroscopic materials, Nature 382 (1996) 607–609.
[24] A. Laromaine, L. Koh, M. Murugesan, R.V. Ulijn, M.M. Stevens, Protease-triggered dispersion of nanoparticle assemblies, J. Am. Chem. Soc. 129 (2007) 4156–4157.
[25] M. Daniel, D. Astruc, Gold nanoparticles: assembly, supramolecular chemistry, quantum-size-related properties, and applications toward biology, catalysis, and nanotechnology, Chem. Rev. 104 (2004) 293–346.
[26] C. Burda, X. Chen, R. Narayanan, M.A. El-Sayed, Chemistry and properties of nanocrystals of different shapes, Chem. Rev. 105 (2005) 1025–1102.
[27] C.S. Purohit, A.K. Mishra, S. Verma, Four-stranded coordination helices containing silver-adenine (purine) metallaquartets, Inorg. Chem. 46 (2007) 8493–8495.
[28] C.S. Purohit, S. Verma, A luminescent silver-adenine metallamacrocyclic quartet, J. Am. Chem. Soc. 128 (2006) 400–401.
[29] C.S. Purohit, S. Verma, Patterned deposition of a mixed-coordination adenine-silver helicate, containing a π-stacked metallacycle, on a graphite surface, J. Am. Chem. Soc. 129 (2007) 3488–3489.
[30] A.K. Mishra, R.K. Prajapati, S. Verma, Probing structural consequences of N9-alkylation in silver-adenine frameworks, Dalton Trans. 39 (2010) 10034–10037.
[31] E. Papadopoulou, S.E.J. Bell, Structure of adenine on metal nanoparticles: pH equilibria and formation of Ag^+ complexes detected by surface-enhanced Raman spectroscopy, J. Phys. Chem. C 114 (2010) 22644–22651.
[32] D. Hunziker, P. Wyss, P. Angehrn, A. Mueller, H. Marty, R. Halm, L. Kellenberger, V. Bitsch, G. Biringer, W. Arnold, Novel ketolide antibiotics with a fused five-membered lactone ring – synthesis, physicochemical and antimicrobial properties, Biorg. Med. Chem. 12 (2004) 3503–3519.
[33] G. Socrates, Infrared and Raman Characteristic Group Frequencies: Tables and Charts, third ed., John Wiley & Sons, Chichester, 2004.
[34] Y.H. Lin, W.L. Tseng, Highly sensitive and selective detection of silver ions and silver nanoparticles in aqueous solution using an oligonucleotide-based fluorogenic probe, Chem. Commun. (2009) 6619–6621.
[35] L. Liu, G. Zhang, J. Xiang, D. Zhang, D. Zhu, Fluorescence "turn on" chemosensors for Ag^+ and Hg^{2+} based on tetraphenylethylene motif featuring adenine and thymine moieties, Org. Lett. 10 (2008) 4581–4584.
[36] M. Kim, Y. Cho, S. Park, Y. Huh, Facile synthesis and fine morphological tuning of Ag_2O, Cryst. Growth Des. 12 (2012) 4180–4185.

Biographies

Yi-Ming Sung is studying for PhD in the Department of Applied Chemistry at National Chiao Tung University.

Shu-Pao Wu had finished PhD in 2004, Department of Chemistry, The Ohio State University, USA. Currently, he is working as an Associate Professor in Department of Applied Chemistry National Chiao Tung University, Taiwan, Republic of China. His current interests are metal ion chemosensors and AlkB.